

## Supplementary Materials for

### **The whole-soil carbon flux in response to warming**

Caitlin E. Hicks Pries,\* C. Castanha, R. C. Porras, M. S. Torn\*

\*Corresponding author. Email: [cehpries@lbl.gov](mailto:cehpries@lbl.gov) (C.E.H.P.); [mstorn@lbl.gov](mailto:mstorn@lbl.gov) (M.S.T.)

Published 9 March 2017 on *Science* First Release  
DOI: 10.1126/science.aal1319

#### **This PDF file includes:**

Materials and Methods

Supplementary Text

Figs. S1 to S6

Tables S1 and S2

Captions for tables S3 to S5

References

#### **Other supplementary material for this manuscript includes the following:**

Tables S3 to S5 (Excel format)

## **Materials and Methods**

### Field Experiment

The University of California Blodgett Experimental Forest is located in the foothills of the Sierra Nevada near Georgetown, CA at 1370 m above sea level. Mean annual precipitation is 1774 mm with most of it occurring from November through April. Mean annual temperature is about 12.5°C (34). The experiment is in a thinned 80 year-old stand of mixed conifers including ponderosa pine (*Pinus ponderosa*), sugar pine (*Pinus lambertiana*), incense cedar (*Calocedrus decurrens*), white fir (*Abies concolor*), and douglas fir (*Pseudotsuga menziesii*). The soils are Alfisols of granitic origin with a developed O horizon (35).

The warming treatment warmed the soil +4°C to 1 m depth while maintaining the natural temperature gradient with depth following the design of Hanson et al. (3). There were three plot pairs consisting of 3 m diameter circular plots—one control and one heated. Twenty-two 2.4 m long steel pipes surrounded each plot, at 0.25 m beyond the plot perimeter to mitigate potential hot spots near the heaters. In heated plots, resistance heater cable (BriskHeat, Ohio, USA) was placed inside the pipes, which were then filled with sand. Steel pipes around the control plots contained sand only. We installed two concentric rings of heater cable at 1 and 2 m in diameter, 5 cm below the soil surface, to compensate for surface heat loss. Unheated cables were installed similarly in control plots. Power to the heaters was routed through silicon-controlled rectifiers (SCRs, Watlow, Missouri, USA) controlled by a CR1000 datalogger (Campbell Scientific, Utah, USA) through a current-to-voltage converter (SDM-CVO4, Campbell Scientific, Utah, USA). The amount of power supplied to the deep heaters was based on the temperature difference between paired control and heated thermistors at 75 and 100 cm depth at a radial distance of 0.75 m from plot center. Power supplied to the surface heaters was based on the temperature difference of thermistors at 15 and 20 cm depth at a radial distance of 0 and 0.75 m from plot center.

### Field Measurements

Dataloggers (CR1000, Campbell Scientific, Utah, USA) continuously recorded soil temperature and moisture at 30 min intervals. Temperature was monitored at 5, 15, 30, 50, 75, and 100 cm depths at a radial distance of 0.75 m from the center of each plot. Heated plots had three additional probes that monitored temperature at 15, 30, 50, and 75 cm at 0, 0.75, and 1.25 m from plot center, while control plots had one similar probe at 0.75 m from plot center. Temperature probes consisted of thermistors (Omega 44005) epoxied to PVC rods, placed inside thin-walled steel conduit with steel tips, which allowed them to be driven into the soil profile. To monitor soil moisture, we used an enviroSCAN (Sentek, Australia) probe fitted with capacitance sensors at 10, 30, 50, and 90 cm at a radial distance of 0.75 m from the center of each plot. We calibrated the soil moisture measurements by comparing the sensor values at each depth to the volumetric water content measured in nearby (within 0.5 m) soil cores. We repeated this sampling five times over two and a half years, in both dry and wet periods.

Surface soil respiration measurements were made approximately monthly from March 2014 through February 2016 using a cavity ring down spectrometer (CRDS, Picarro, Santa Clara, California). An opaque chamber (14.4 cm tall by 10 cm in diameter) connected to the CRDS was placed on 10 cm diameter by 10 cm tall PVC collars for four

to six minutes depending on the flux rate. Each plot had seven collars permanently embedded to a depth of 5 cm. Soil temperature at 10 cm was measured with a thermocouple probe (Hanna, Italy) during each flux measurement. Additionally, soil respiration autochambers (8100A, LI-COR, Lincoln, Nebraska) measured soil respiration fluxes every 30-60 minutes in each plot throughout the experiment. The autochamber data showed that variation in fluxes diurnally ( $SD=0.3 \text{ umol m}^{-2} \text{ s}^{-1}$ ) and daily ( $SD=0.9 \text{ umol m}^{-2} \text{ s}^{-1}$ ) was small compared to the average flux rates ( $3.6-4 \text{ umol m}^{-2} \text{ s}^{-1}$ ) and did not differ between heated and control treatments. Our monthly sampling with its greater spatial resolution was therefore temporally representative enough to be scaled up for annual flux estimates.

To model how  $\text{CO}_2$  production changes with depth and warming, each plot had a set of gas wells at 15, 30, 50, 75, and 90 cm. The gas wells were 6.35 mm diameter stainless steel tubes inserted into the soil at a  $45^\circ$  angle to the desired depth and topped with straight swage pipefittings (Swagelok Ohio, USA) with septa. On the same days as the surface soil respiration measurements, samples were collected from the wells with a syringe. After clearing the headspace in each well, a 25 ml gas sample was transferred to an evacuated 20 ml septa-topped glass vial. For analysis, 5 ml samples were injected into the small sample isotope module of a Picarro CRDS where they were diluted with ultra zero air (without  $\text{CO}_2$ ). A four-point calibration curve ranging from 2,000 to 20,000 ppm was used to calculate the  $\text{CO}_2$  concentration from the CRDS data.

$\text{CO}_2$  production from each depth section was modeled using soil depth profile  $\text{CO}_2$  concentration, moisture, and temperature data and Fick's Law of Diffusion following (36):

$$F = -D \frac{dC}{dz}$$

Where  $F$  is the  $\text{CO}_2$  flux density across a horizontal plane at each soil depth ( $\text{umol m}^{-2} \text{ s}^{-1}$ ),  $dC/dz$  is the change in  $\text{CO}_2$  mol fraction at the soil surface and each depth (calculated using the first derivative of a curve fit to the  $\text{CO}_2$  mol fraction depth profile), and  $D$  is the diffusion coefficient ( $\text{mm}^2 \text{ s}^{-1}$ ). The diffusion coefficient is calculated using:

$$D = D_o * \xi$$

Where  $D_o$  is the diffusion coefficient of  $\text{CO}_2$  in air at the soil temperature and local air pressure and  $\xi$  is the dimensionless tortuosity factor. We estimated tortuosity using 6 different equations (36-39) and chose the equation that gave the best match between the surface flux estimated from the soil profile data and the measured surface flux. The equation that worked best was an empirical relationship from (36):

$$\xi = 0.95\varepsilon^{1.93}$$

Where  $\varepsilon$  is the air-filled porosity ( $\text{m}^3 \text{ m}^{-3}$ ) calculated from the total soil porosity and volumetric water content at each soil depth and time of measurement.  $\text{CO}_2$  production ( $\text{umol m}^{-3} \text{ s}$ ) from a given depth interval was calculated by subtracting the difference in flux densities across that interval and dividing by the depth increment.

In late February 2015, we collected soil air at 15, 50, and 90 cm for radiocarbon analysis. One liter of air was collected from 15 cm depths and 0.5 L of air was collected from 50 and 90 cm depths from each control and heated plot into evacuated stainless steel canisters.  $\text{CO}_2$  from each canister was purified on a vacuum line and reduced to graphite by Fe reduction in  $\text{H}_2$  (40). The graphite was measured by Accelerator Mass Spectrometry (AMS) at Lawrence Livermore National Laboratory (LLNL).

In early March 2015, we collected a soil core near each plot pair. Soils from 10-20, 45-55, and 85-95 cm depths had roots removed and were placed into mason jars. After 10 days incubating at 20°C, the headspace was scrubbed of CO<sub>2</sub> and allowed to build up over 10 days before being collected into evacuated stainless steel canisters and processed for <sup>14</sup>C analysis as described above.

#### Soil Characterization

To characterize the soils, we dug three 1 m-deep soil pits in the same forest stand as the experiment. Soil horizons were characterized according to the NRCS field book (USDA, 2012), and in all pits the lowest depth (1 m) was within the BC horizon. We sampled for bulk density using a hammer corer (10 cm long by 5.35 cm diameter) in the center of each soil horizon. For all other analyses, soils were channel-sampled every 10 cm to a depth of 1 m. Soils were sieved through a 2 mm mesh and split into subsamples to be freeze-dried or analyzed for pH. Subsamples of the freeze-dried soils were ground and run on an EA-IRMS (IsoPrime 100 IRMS in line with a Vario micro cube EA, Isoprime, United Kingdom) for %C, %N, and δ<sup>13</sup>C. For 10-20, 50-60, and 90-100 cm depths, a second subsample was analyzed for bulk <sup>14</sup>C and a third was density-separated into free light, occluded light, and dense fractions using a 1.7 g ml<sup>-1</sup> sodium polytungstate solution and methods refined in our lab (41-43). The resulting soil fractions were analyzed for C, N, and <sup>14</sup>C (except for the occluded fraction, which was too small for <sup>14</sup>C analysis). For <sup>14</sup>C analysis, organic carbon was oxidized to CO<sub>2</sub> by sealed-tube combustion with cupric oxide and then graphitized and analyzed at the LLNL AMS as above.

#### Data Analysis

The apparent Q<sub>10</sub> was calculated using the following equation for each pair of control and heated plots:

$$Q_{10} = \frac{R_H}{R_C}^{10/(T_H - T_C)}$$

Where R<sub>H</sub> and R<sub>C</sub> are the CO<sub>2</sub> production rates of the heated and control plots, respectively, and T<sub>H</sub> and T<sub>C</sub> are the temperatures of the heated and control plots, respectively. For surface production, we used the soil temperature at 10 cm measured during the flux. For production from each soil depth, we used the mean plot soil temperature at the middle of each depth layer at the time of sample collection. Due to California's Mediterranean climate in which high soil temperatures are correlated with low soil moisture (Figure S4), we were unable to fit a temperature curve that would have allowed us to calculate an apparent Q<sub>10</sub> as in (44), or fit an activation energy from an Arrhenius function (45), or tease apart temperature and moisture effects (Figure S4). By using a direct comparison between control and heated plots to calculate Q<sub>10</sub> and not fitting a curve, we avoided problems with Q<sub>10</sub> model behavior wherein trends can be erroneously fit to random numbers as demonstrated by (45) and we avoided mistakenly attributing temperature responses to confounding seasonal trends of substrate or moisture availability. However, the direct calculation led to high variability because spatial heterogeneity in substrate availability and microbial activity between control and heated pairs could not be controlled. Thus, we excluded unrealistic values (Q<sub>10</sub> > 30); as a result 10% of the data were excluded. Also, given the slight drying in the heated plots that could reduce the respiration response, this direct calculation may underestimate temperature sensitivity.

To test the effect of warming on CO<sub>2</sub> production at the surface, CO<sub>2</sub> production within soil depth intervals, and Q<sub>10</sub>, we built mixed effects models using the lme4 package in R (46, 47) using restricted maximum likelihood with treatment, depth (where applicable), and two-way interactions as fixed effects. We tested whether random effects, variance structures, and temporal autocorrelation structures improved model AIC following (48). For surface production, respiration collar location nested in plot was included as a random effect, and for production within depths, depth nested in plot was included as a random effect. Both models used sampling date as a random effect and included a variance structure, which was based on plot (surface CO<sub>2</sub> production) or depth (within-depth CO<sub>2</sub> production). For Q<sub>10</sub> of within-depth production, depth nested in replicate was the random effect and depth was included in the variance structure. We also tested whether Q<sub>10</sub> changed over time by running a linear regression with months since warming began as the predictor and depth nested in replicate as a random effect. Residuals of the final models were graphically checked to ensure model assumptions were met.

## Supplementary Text

There are several lines of evidence that point to heterotrophic respiration being the dominant contributor to soil respiration, particularly at depth. First, the fine (<2 cm) root C pool (to 1 m) is only 7% the size of the SOC pool and 25% of the free, non mineral-associated OC pool. Second, root contributions to soil respiration were found to correlate with fine root distributions with roots contributing 50% to O horizon soil respiration but only 25% to soil respiration at 20 cm in a temperate forest soil (49). At our site, fine root density was low in subsoils (Fig. S6), so the majority of subsoil respiration was likely heterotrophic. Lastly, as discussed in the paper, the radiocarbon values of soil profile CO<sub>2</sub> (40.9‰) were closer to free light fraction SOC (35.9‰) and root-free incubations (42.5‰) than to the atmosphere, which is the source of recent photosynthate and thus root respiration. Assuming 3-4‰ per year decreases in Δ<sup>14</sup>C since the last published atmospheric Δ<sup>14</sup>C values in 2009 (50), the Δ<sup>14</sup>C of root respiration should be around 21-27‰, which is more depleted than the soil profile <sup>14</sup>CO<sub>2</sub>. We only sampled for radiocarbon in February, but that was during the time of year with the strongest soil respiration response to warming.

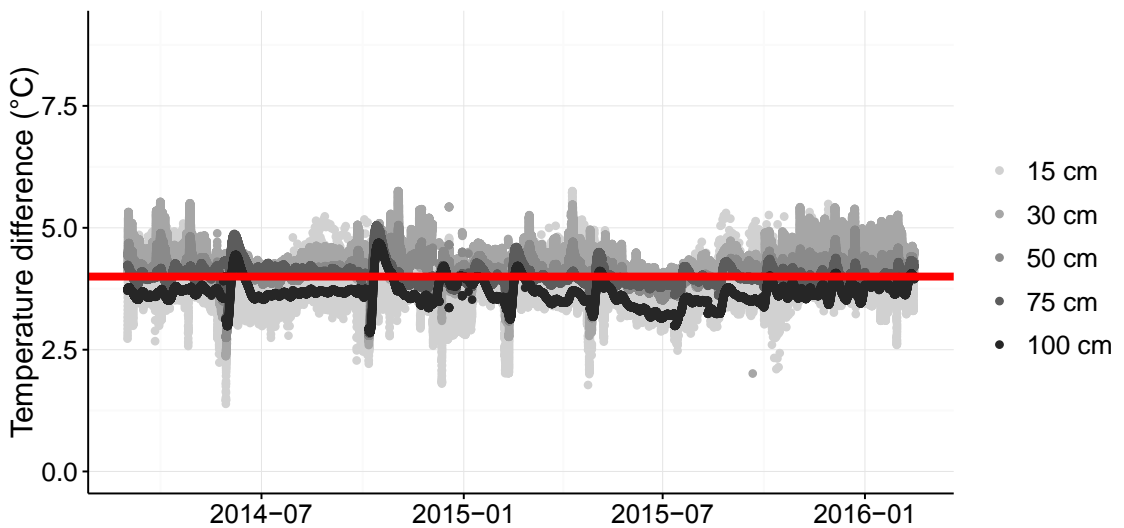


**Fig. S1.**

The average temperature difference between the control and heated plots at five depths over the study period (March 2014 through February 2015). The red line is the +4°C target. Discontinuities in warming (drops followed by sharp increases) were due to electrical outages.

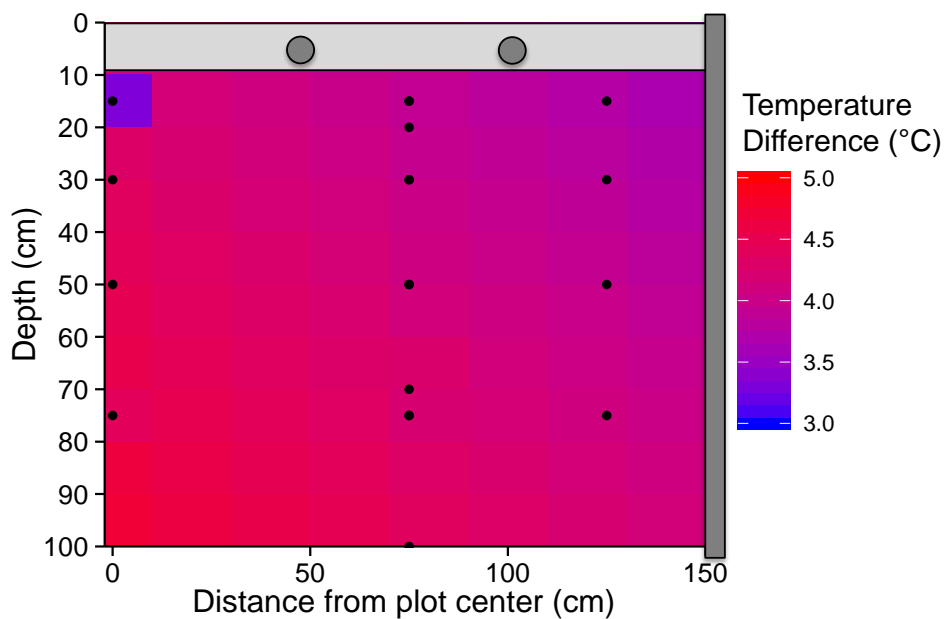


**Fig. S2**

A radial cross-section of plot 1, (representative of plots 2 and 3, not shown), showing the average temperature difference during December 2014. The black dots represent the location of temperature sensors. The grey circles are the location of the surface heaters and the vertical grey bar represents the 2.4 m long deep heaters, which are located 25 cm from the edge of the plot at 175 cm from plot center. The data were interpolated using the automap package in R.

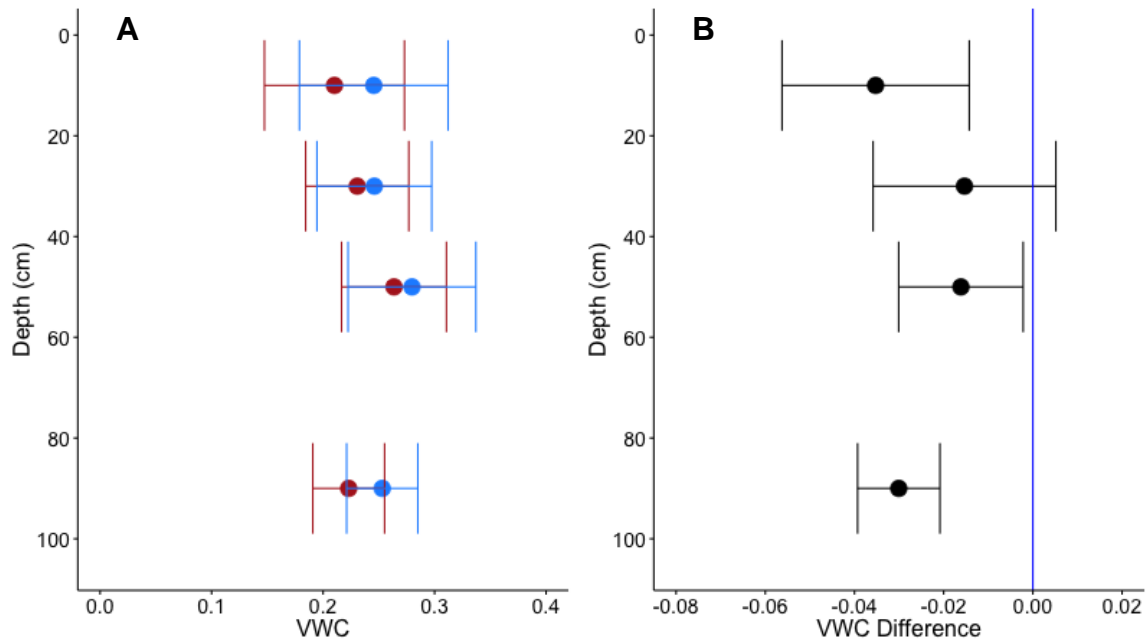


**Fig. S3**

The average soil moisture (volumetric water content) in the heated (red) and control (blue) plots (Left) and the average difference (heated-control; Right) for the time period studied (March 2014 through February 2016). The standard deviation represents the temporal variation.

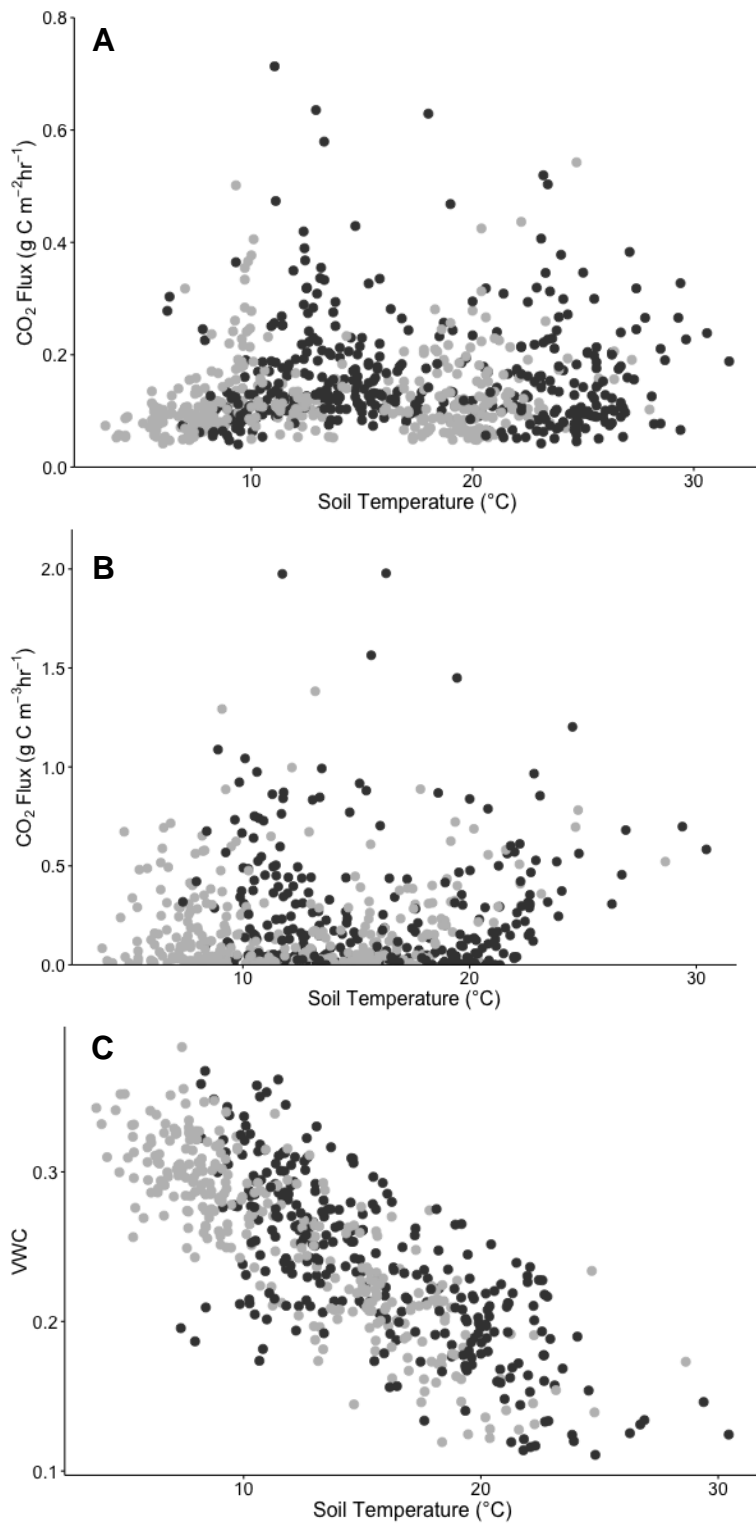


**Fig. S4**

There was no relationship between either (A) surface CO<sub>2</sub> production and soil temperature or (B) CO<sub>2</sub> production from individual depths and soil temperature at that depth. This lack of relationship was due to (C) the strong negative correlation ( $r=-0.8$ )

between soil temperature and moisture. The light grey circles are data from the control plots and the dark grey circles are data from the heated plots.

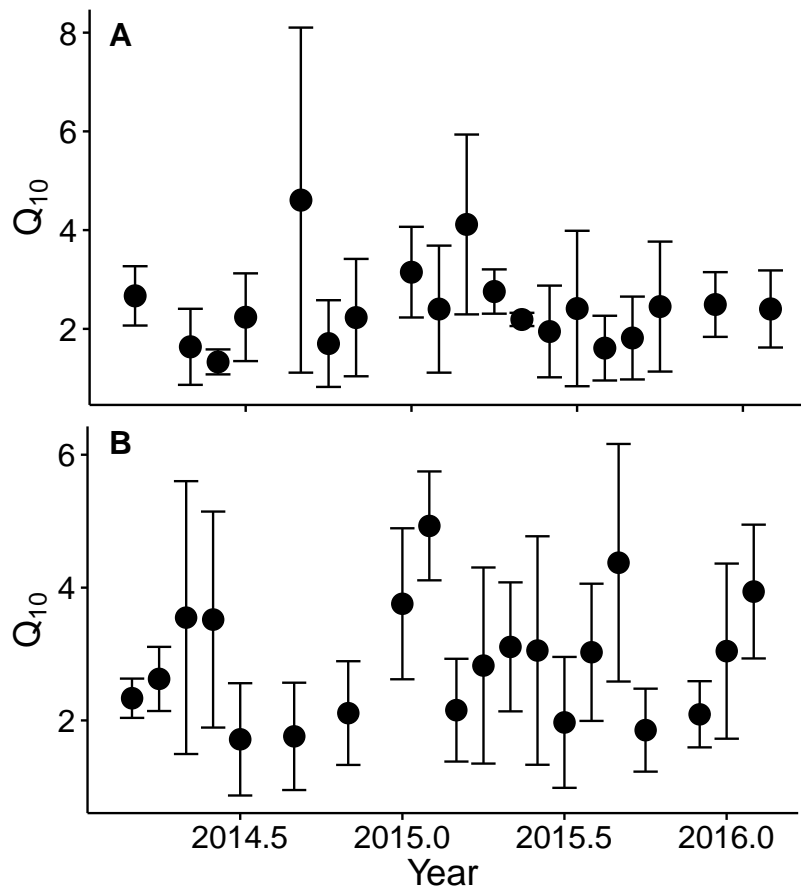


**Fig. S5**

The mean  $Q_{10}$  of surface production (A) and production within depth increments (B) by time since warming was initiated at the end of October 2013. The error bars represent the standard error. There was no significant decline in  $Q_{10}$  over time for either the surface or within depths (regression with plot as a random effect,  $p=0.66$ ; regression with depth increment within replicate as a random effect,  $p=0.51$ ).

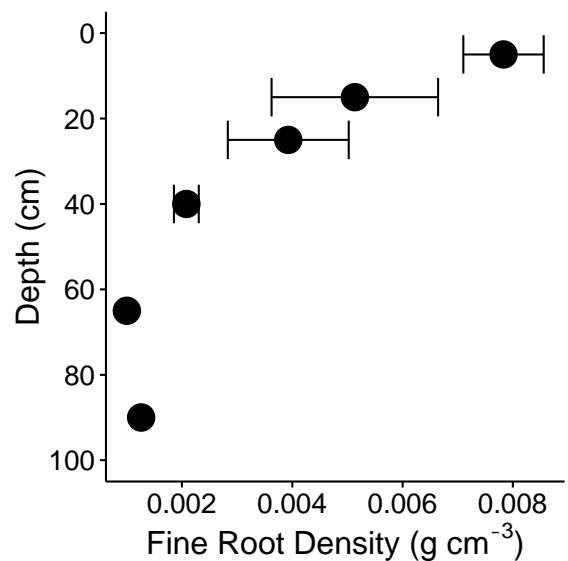


**Fig. S6**

Mean fine root density ( $\pm \text{SE}$ ) with soil depth.

**Table S1.**

Response of soil respiration to warming in non-permafrost soils by warming method and measured warming depth.

Ecosystem Type	Location	Heating Method <sup>1</sup>	Measurement Depth (cm)	Soil Warming (°C)	Soil Respiration Δ	Citation
Alpine Meadow	CO, USA	AG infrared	5-25	0-1.4	No effect	(51, 52)
Alpine Meadow	CHN	AG infrared	0-40	0.5-1.5, 0.5 at depth	9.2%	(53, 54)
Grassland	OK, USA	AG infrared	2.5 (10) <sup>2</sup>	2-2.6	No effect	(55)
Grassland	OK, USA	AG infrared	5	1.4-2.0	9-15.6%	(56)
Grassland	OK, USA	AG infrared	2.5	1.7-2.2	8-15%	(57)
Grassland	OK, USA	AG infrared	2.5	2	≈20%	(58)
Old Field	MA, USA	AG infrared	5	1, 2.3, 3.5	No effect <sup>4</sup>	(59)
Steppe	Inner Mongolia, CHN	AG infrared	10	0.6-1.8	-4.5%	(60)
Boreal Forest	AK, USA	CTGs	5	0.5	-22%	(61)
Boreal Forest	Ilomantsi, FIN	CTGs	2	2-4	27-43%	(62)
Boreal Forest	Flakaliden, SWE	Large CTGs	10	0	No effect	(63)
Old Field	TN, USA	OTCs w/ heaters	5	1.1-1.8	-11.7%-0	(64, 65)
Forest-Steppe	HUN	NI	1	1.5 at dawn	-13.5%	(66)
Shrubland	DEN, GBR, NLD, ESP	NI	0-10	0.5-1.1	No effect	(67, 68)
Alpine Forest	AUS	BC (3 cm)	5	4	33-40%	(69)
Boreal Forest	ME, USA	BC (1-2 cm)	0-50	5, 3 at depth	25-40%	(70)
Boreal Forest	Manitoba, CAN	BC (10 cm), CTGs w/ heaters	10 (100) <sup>3</sup>	5	11-24%	(71)
Deciduous Forest	NY, USA	BC (5 cm)	5	2.5, 5.0, 7.5	19-58%	(72)
Deciduous Forest	MA, USA	BC (10 cm)	not specified	5	44% <sup>5</sup>	(73)
Deciduous Forest	MA, USA	BC (10 cm)	not specified	5	28% years 0-6, 5% years 7-10	(31, 74)
Deciduous Forest	MA, USA	BC (10 cm)	not specified	5	35% year 1, 15% year 7	(75)
Deciduous Forest	MA, USA	BC (10 cm)	20 (100) <sup>2</sup>	5	60%	(76)
Deciduous Forest	TN, USA	Vertical rods, AGI	200	4	Increased <sup>6</sup>	(17)
Garden	York, GBR	SC in grid	4	3	0-25%	(77)
Grassland	Cumbria, GBR	SC in grid	2-20	3, 1 at depth	Not reported	(78)

<sup>1</sup>AG=Aboveground, CTG=Closed top greenhouse, OTC=Open top chamber, NI=Nighttime insulation, BC=Buried cable, SC=Surface Cable<sup>2</sup>A one-time measurement, <sup>3</sup>Result of temperature not reported, <sup>4</sup>Heterotrophic respiration only, <sup>5</sup>During spring and fall only, <sup>6</sup>Magnitude not reported

**Table S2.**

Fixed effect coefficients and significance from mixed model regressions run using the lmer command in R.

<b>Response</b>	<b># obs</b>	<b>Coefficients</b>	<b>Estimate</b>	<b>SE</b>	<b>t-value</b>	<b>P-value</b>
CO2 production by depth (umol C m <sup>-2</sup> s <sup>-1</sup> )	590	Intercept	9.9	1.3	7.75	<0.0001
		Treatment	4.1	1.8	2.26	0.03
		Depth	-0.14	0.025	-5.5	<0.0001
		Depth*Treatment	-0.06	0.035	-1.7	0.10
CO2 production from surface (g C m <sup>-2</sup> h <sup>-1</sup> )	820	Intercept (Control)	0.12	0.02	5.11	0.009
		Heated	0.048	0.01	4.99	<0.0001
Q <sub>10</sub>	263	Intercept	4.3	0.98	4.42	0.001
		Depth	-0.03	0.018	-1.95	0.08

### **Additional Data Table S3 (separate file)**

SurfaceFlux.csv contains the CO<sub>2</sub> production from the soil surface for all the collars within each plot for each month sampled and the corresponding soil temperature at 10 cm (°C) and volumetric water content at 10 cm (%).

### **Additional Data Table S4 (separate file)**

WithinDepthFlux.csv contains the CO<sub>2</sub> production (g C m<sup>-3</sup> hr<sup>-1</sup>) data within each depth increment for each plot and month sampled and also includes the corresponding soil temperature (°C) and volumetric water content (%).

### **Additional Data Table S5 (separate file)**

SoilFrac14C.csv contains the data from the density fractionations, including the proportion of the carbon in free light and dense fractions and the Δ<sup>14</sup>C in ‰.

## References

1. M. Köchy, R. Hiederer, A. Freibauer, Global distribution of soil organic carbon—Part 1: Masses and frequency distributions of SOC stocks for the tropics, permafrost regions, wetlands, and the world. *Soil* **1**, 351–365 (2015). [doi:10.5194/soil-1-351-2015](https://doi.org/10.5194/soil-1-351-2015)
2. M. W. Schmidt, M. S. Torn, S. Abiven, T. Dittmar, G. Guggenberger, I. A. Janssens, M. Kleber, I. Kögel-Knabner, J. Lehmann, D. A. C. Manning, P. Nannipieri, D. P. Rasse, S. Weiner, S. E. Trumbore, Persistence of soil organic matter as an ecosystem property. *Nature* **478**, 49–56 (2011). [doi:10.1038/nature10386](https://doi.org/10.1038/nature10386) [Medline](#)
3. E. G. Jobbágy, R. B. Jackson, The vertical distribution of soil organic carbon and its relation to climate and vegetation. *Ecol. Appl.* **10**, 423–436 (2000). [doi:10.1890/1051-0761\(2000\)010\[0423:TVDOSO\]2.0.CO;2](https://doi.org/10.1890/1051-0761(2000)010[0423:TVDOSO]2.0.CO;2)
4. M. Reichstein, C. Beer, Soil respiration across scales: The importance of a model-data integration framework for data interpretation. *J. Plant Nutr. Soil Sci.* **171**, 344–354 (2008). [doi:10.1002/jpln.200700075](https://doi.org/10.1002/jpln.200700075)
5. T. W. Crowther, K. E. O. Todd-Brown, C. W. Rowe, W. R. Wieder, J. C. Carey, M. B. Machmuller, B. L. Snoek, S. Fang, G. Zhou, S. D. Allison, J. M. Blair, S. D. Bridgman, A. J. Burton, Y. Carrillo, P. B. Reich, J. S. Clark, A. T. Classen, F. A. Dijkstra, B. Elberling, B. A. Emmett, M. Estiarte, S. D. Frey, J. Guo, J. Harte, L. Jiang, B. R. Johnson, G. Kröel-Dulay, K. S. Larsen, H. Laudon, J. M. Lavallee, Y. Luo, M. Lupascu, L. N. Ma, S. Marhan, A. Michelsen, J. Mohan, S. Niu, E. Pendall, J. Peñuelas, L. Pfeifer-Meister, C. Poll, S. Reinsch, L. L. Reynolds, I. K. Schmidt, S. Sistla, N. W. Sokol, P. H. Templer, K. K. Treseder, J. M. Welker, M. A. Bradford, Quantifying global soil carbon losses in response to warming. *Nature* **540**, 104–108 (2016). [doi:10.1038/nature20150](https://doi.org/10.1038/nature20150) [Medline](#)
6. A. A. Berhe, J. W. Harden, M. S. Torn, J. Harte, Linking soil organic matter dynamics and erosion-induced terrestrial carbon sequestration at different landform positions. *J. Geophys. Res.* **113**, G04039 (2008). [doi:10.1029/2008JG000751](https://doi.org/10.1029/2008JG000751)
7. K. Eusterhues, C. Rumpel, M. Kleber, I. Kögel-Knabner, Stabilisation of soil organic matter by interactions with minerals as revealed by mineral dissolution and oxidative degradation. *Org. Geochem.* **34**, 1591–1600 (2003). [doi:10.1016/j.orggeochem.2003.08.007](https://doi.org/10.1016/j.orggeochem.2003.08.007)
8. C. Rumpel, I. Kögel-Knabner, Deep soil organic matter—a key but poorly understood component of terrestrial C cycle. *Plant Soil* **338**, 143–158 (2011). [doi:10.1007/s11104-010-0391-5](https://doi.org/10.1007/s11104-010-0391-5)
9. J. Koarashi, W. C. Hockaday, C. A. Masiello, S. E. Trumbore, Dynamics of decadally cycling carbon in subsurface soils. *J. Geophys. Res.* **117**, G03033 (2012). [doi:10.1029/2012JG002034](https://doi.org/10.1029/2012JG002034)

10. E. A. Davidson, I. A. Janssens, Temperature sensitivity of soil carbon decomposition and feedbacks to climate change. *Nature* **440**, 165–173 (2006). [doi:10.1038/nature04514](https://doi.org/10.1038/nature04514) [Medline](#)
11. J. Gillabel, B. Cebrian-Lopez, J. Six, R. Merckx, Experimental evidence for the attenuating effect of SOM protection on temperature sensitivity of SOM decomposition. *Glob. Change Biol.* **16**, 2789–2798 (2010). [doi:10.1111/j.1365-2486.2009.02132.x](https://doi.org/10.1111/j.1365-2486.2009.02132.x)
12. C. Salomé, N. Nunan, V. Pouteau, T. Z. Lerch, C. Chenu, Carbon dynamics in topsoil and in subsoil may be controlled by different regulatory mechanisms. *Glob. Change Biol.* **16**, 416–426 (2010). [doi:10.1111/j.1365-2486.2009.01884.x](https://doi.org/10.1111/j.1365-2486.2009.01884.x)
13. N. Fierer, A. S. Allen, J. P. Schimel, P. A. Holden, Controls on microbial CO<sub>2</sub> production: A comparison of surface and subsurface soil horizons. *Glob. Change Biol.* **9**, 1322–1332 (2003). [doi:10.1046/j.1365-2486.2003.00663.x](https://doi.org/10.1046/j.1365-2486.2003.00663.x)
14. C.-E. Gabriel, L. Kellman, Investigating the role of moisture as an environmental constraint in the decomposition of shallow and deep mineral soil organic matter of a temperate coniferous soil. *Soil Biol. Biochem.* **68**, 373–384 (2014). [doi:10.1016/j.soilbio.2013.10.009](https://doi.org/10.1016/j.soilbio.2013.10.009)
15. H. Eswaran, E. Van Den Berg, P. Reich, Organic carbon in soils of the world. *Soil Sci. Soc. Am. J.* **57**, 192–194 (1993). [doi:10.2136/sssaj1993.03615995005700010034x](https://doi.org/10.2136/sssaj1993.03615995005700010034x)
16. IPCC, *Climate Change 2013: The Physical Science Basis. Contribution of Working Group I to the Fifth Assessment Report of the Intergovernmental Panel on Climate Change* (Cambridge Univ. Press, 2013); [www.ipcc.ch/report/ar5/wg1/](http://www.ipcc.ch/report/ar5/wg1/).
17. P. J. Hanson, K. W. Childs, S. D. Wullschleger, J. S. Riggs, W. K. Thomas, D. Todd, J. M. Warren, A method for experimental heating of intact soil profiles for application to climate change experiments. *Glob. Change Biol.* **17**, 1083–1096 (2011). [doi:10.1111/j.1365-2486.2010.02221.x](https://doi.org/10.1111/j.1365-2486.2010.02221.x)
18. J. W. Raich, W. H. Schlesinger, The global carbon dioxide flux in soil respiration and its relationship to vegetation and climate. *Tellus B* **44**, 81–99 (1992). [doi:10.3402/tellusb.v44i2.15428](https://doi.org/10.3402/tellusb.v44i2.15428)
19. B. Bond-Lamberty, A. Thomson, A global database of soil respiration data. *Biogeosciences* **7**, 1915–1926 (2010). [doi:10.5194/bg-7-1915-2010](https://doi.org/10.5194/bg-7-1915-2010)
20. J. C. Carey, J. Tang, P. H. Templer, K. D. Kroeger, T. W. Crowther, A. J. Burton, J. S. Dukes, B. Emmett, S. D. Frey, M. A. Heskel, L. Jiang, M. B. Machmuller, J. Mohan, A. M. Panetta, P. B. Reich, S. Reinsch, X. Wang, S. D. Allison, C. Bamminger, S. Bridgham, S. L. Collins, G. de Dato, W. C. Eddy, B. J. Enquist, M. Estiarte, J. Harte, A. Henderson, B. R. Johnson, K. S. Larsen, Y. Luo, S. Marhan, J. M. Melillo, J. Peñuelas, L. Pfeifer-Meister, C. Poll, E. Rastetter, A. B. Reinmann, L. L. Reynolds, I. K. Schmidt, G. R. Shaver, A. L. Strong, V. Suseela, A. Tietema, Temperature response of soil respiration

largely unaltered with experimental warming. *Proc. Natl. Acad. Sci. U.S.A.* **113**, 13797–13802 (2016). [doi:10.1073/pnas.1605365113](https://doi.org/10.1073/pnas.1605365113) Medline

21. M. Lu, X. Zhou, Q. Yang, H. Li, Y. Luo, C. Fang, J. Chen, X. Yang, B. Li, Responses of ecosystem carbon cycle to experimental warming: A meta-analysis. *Ecology* **94**, 726–738 (2013). [doi:10.1890/12-0279.1](https://doi.org/10.1890/12-0279.1) Medline
22. Z. Wu, P. Dijkstra, G. W. Koch, J. Peñuelas, B. A. Hungate, Responses of terrestrial ecosystems to temperature and precipitation change: A meta-analysis of experimental manipulation. *Glob. Change Biol.* **17**, 927–942 (2011). [doi:10.1111/j.1365-2486.2010.02302.x](https://doi.org/10.1111/j.1365-2486.2010.02302.x)
23. X. Pang, B. Zhu, X. Lü, W. Cheng, Labile substrate availability controls temperature sensitivity of organic carbon decomposition at different soil depths. *Biogeochemistry* **126**, 85–98 (2015). [doi:10.1007/s10533-015-0141-0](https://doi.org/10.1007/s10533-015-0141-0)
24. C. D. Koven, W. J. Riley, Z. M. Subin, J. Y. Tang, M. S. Torn, W. D. Collins, G. B. Bonan, D. M. Lawrence, S. C. Swenson, The effect of vertically resolved soil biogeochemistry and alternate soil C and N models on C dynamics of CLM4. *Biogeosciences* **10**, 7109–7131 (2013). [doi:10.5194/bg-10-7109-2013](https://doi.org/10.5194/bg-10-7109-2013)
25. D. S. Jenkinson, K. Coleman, The turnover of organic carbon in subsoils. Part 2. Modelling carbon turnover. *Eur. J. Soil Sci.* **59**, 400–413 (2008). [doi:10.1111/j.1365-2389.2008.01026.x](https://doi.org/10.1111/j.1365-2389.2008.01026.x)
26. K. E. O. Todd-Brown, J. T. Randerson, W. M. Post, F. M. Hoffman, C. Tarnocai, E. A. G. Schuur, S. D. Allison, Causes of variation in soil carbon simulations from CMIP5 Earth system models and comparison with observations. *Biogeosciences* **10**, 1717–1736 (2013). [doi:10.5194/bg-10-1717-2013](https://doi.org/10.5194/bg-10-1717-2013)
27. C. L. Phillips, K. J. McFarlane, D. Risk, A. R. Desai, Biological and physical influences on soil  $^{14}\text{CO}_2$  seasonal dynamics in a temperate hardwood forest. *Biogeosciences* **10**, 7999–8012 (2013). [10.5194/bg-10-7999-2013](https://doi.org/10.5194/bg-10-7999-2013)
28. E. A. Davidson, S. E. Trumbore, Gas diffusivity and production of  $\text{CO}_2$  in deep soils of the eastern Amazon. *Tellus B* **47**, 550–565 (1995). [doi:10.3402/tellusb.v47i5.16071](https://doi.org/10.3402/tellusb.v47i5.16071)
29. A. H. Goldstein, N. E. Hultman, J. M. Fracheboud, M. R. Bauer, J. A. Panek, M. Xu, Y. Qi, A. B. Guenther, W. Baugh, Effects of climate variability on the carbon dioxide, water, and sensible heat fluxes above a ponderosa pine plantation in the Sierra Nevada (CA). *Agric. For. Meteorol.* **101**, 113–129 (2000). [doi:10.1016/S0168-1923\(99\)00168-9](https://doi.org/10.1016/S0168-1923(99)00168-9)
30. N. Fierer, O. A. Chadwick, S. E. Trumbore, Production of  $\text{CO}_2$  in soil profiles of a California annual grassland. *Ecosystems* **8**, 412–429 (2005). [doi:10.1007/s10021-003-0151-y](https://doi.org/10.1007/s10021-003-0151-y)

31. J. M. Melillo, P. A. Steudler, J. D. Aber, K. Newkirk, H. Lux, F. P. Bowles, C. Catricala, A. Magill, T. Ahrens, S. Morrisseau, Soil warming and carbon-cycle feedbacks to the climate system. *Science* **298**, 2173–2176 (2002). [doi:10.1126/science.1074153](https://doi.org/10.1126/science.1074153) Medline
32. B. Bond-Lamberty, A. Thomson, Temperature-associated increases in the global soil respiration record. *Nature* **464**, 579–582 (2010). [doi:10.1038/nature08930](https://doi.org/10.1038/nature08930) Medline
33. C. Le Quéré, R. M. Andrew, J. G. Canadell, S. Sitch, J. I. Korsbakken, G. P. Peters, A. C. Manning, T. A. Boden, P. P. Tans, R. A. Houghton, R. F. Keeling, S. Alin, O. D. Andrews, P. Anthoni, L. Barbero, L. Bopp, F. Chevallier, L. P. Chini, P. Ciais, K. Currie, C. Delire, S. C. Doney, P. Friedlingstein, T. Gkrizalis, I. Harris, J. Hauck, V. Haverd, M. Hoppema, K. Klein Goldewijk, A. K. Jain, E. Kato, A. Körtzinger, P. Landschützer, N. Lefèvre, A. Lenton, S. Lienert, D. Lombardozzi, J. R. Melton, N. Metzl, F. Millero, P. M. S. Monteiro, D. R. Munro, J. E. M. S. Nabel, S. Nakaoka, K. O'Brien, A. Olsen, A. M. Omar, T. Ono, D. Pierrot, B. Poulter, C. Rödenbeck, J. Salisbury, U. Schuster, J. Schwinger, R. Séférian, I. Skjelvan, B. D. Stocker, A. J. Sutton, T. Takahashi, H. Tian, B. Tilbrook, I. T. van der Laan-Luijkx, G. R. van der Werf, N. Viovy, A. P. Walker, A. J. Wiltshire, S. Zaehle, Global carbon budget 2016. *Earth Syst. Sci. Data* **8**, 605–649 (2016). [doi:10.5194/essd-8-605-2016](https://doi.org/10.5194/essd-8-605-2016)
34. J. A. Bird, M. S. Torn, Fine roots vs. needles: A comparison of  $^{13}\text{C}$  and  $^{15}\text{N}$  dynamics in a ponderosa pine forest soil. *Biogeochemistry* **79**, 361–382 (2006). [doi:10.1007/s10533-005-5632-y](https://doi.org/10.1007/s10533-005-5632-y)
35. C. Rasmussen, M. S. Torn, R. J. Southard, Mineral assemblage and aggregates control carbon dynamics in a California conifer forest. *Soil Sci. Soc. Am. J.* **69**, 1711–1721 (2005). [doi:10.2136/sssaj2005.0040](https://doi.org/10.2136/sssaj2005.0040)
36. A. B. Moyes, D. R. Bowling, Interannual variation in seasonal drivers of soil respiration in a semi-arid Rocky Mountain meadow. *Biogeochemistry* **113**, 683–697 (2013). [doi:10.1007/s10533-012-9797-x](https://doi.org/10.1007/s10533-012-9797-x)
37. R. J. Millington, Gas diffusion in porous media. *Science* **130**, 100–102 (1959). [doi:10.1126/science.130.3367.100-a](https://doi.org/10.1126/science.130.3367.100-a) Medline
38. P. Moldrup, T. Olesen, T. Komatsu, P. Schjønning, D. E. Rolston, Tortuosity, diffusivity, and permeability in the soil liquid and gaseous phases. *Soil Sci. Soc. Am. J.* **65**, 613 (2001). [doi:10.2136/sssaj2001.653613x](https://doi.org/10.2136/sssaj2001.653613x)
39. R. Jassal, A. Black, M. Novak, K. Morgenstern, Z. Nesic, D. Gaumont-Guay, Relationship between soil  $\text{CO}_2$  concentrations and forest-floor  $\text{CO}_2$  effluxes. *Agric. For. Meteorol.* **130**, 176–192 (2005). [doi:10.1016/j.agrformet.2005.03.005](https://doi.org/10.1016/j.agrformet.2005.03.005)
40. J. S. Vogel, D. E. Nelson, J. R. Sounthor,  $^{14}\text{C}$  background levels in an accelerator mass spectrometry system. *Radiocarbon* **29**, 323–333 (1987). [doi:10.1017/S003382200043733](https://doi.org/10.1017/S003382200043733)

41. A. Golchin, J. Oades, J. Skjemstad, P. Clarke, Soil structure and carbon cycling. *Soil Res.* **32**, 1043–1068 (1994). [doi:10.1071/SR9941043](https://doi.org/10.1071/SR9941043)
42. C. W. Swanston, M. S. Torn, P. J. Hanson, J. R. Southon, C. T. Garten, E. M. Hanlon, L. Ganio, Initial characterization of processes of soil carbon stabilization using forest stand-level radiocarbon enrichment. *Geoderma* **128**, 52–62 (2005). [doi:10.1016/j.geoderma.2004.12.015](https://doi.org/10.1016/j.geoderma.2004.12.015)
43. J. A. Bird, M. Kleber, M. S. Torn,  $^{13}\text{C}$  and  $^{15}\text{N}$  stabilization dynamics in soil organic matter fractions during needle and fine root decomposition. *Org. Geochem.* **39**, 465–477 (2008). [doi:10.1016/j.orggeochem.2007.12.003](https://doi.org/10.1016/j.orggeochem.2007.12.003)
44. N. Fierer, J. M. Craine, K. McLauchlan, J. P. Schimel, Litter quality and the temperature sensitivity of decomposition. *Ecology* **86**, 320–326 (2005). [doi:10.1890/04-1254](https://doi.org/10.1890/04-1254)
45. C. A. Sierra, Temperature sensitivity of organic matter decomposition in the Arrhenius equation: Some theoretical considerations. *Biogeochemistry* **108**, 1–15 (2012). [doi:10.1007/s10533-011-9596-9](https://doi.org/10.1007/s10533-011-9596-9)
46. D. Bates, M. Mächler, B. Bolker, S. Walker, Fitting linear mixed-effects models using lme4. *J. Stat. Softw.* **67**, 1–48 (2015). [doi:10.18637/jss.v067.i01](https://doi.org/10.18637/jss.v067.i01)
47. R Development Core Team, *R: A Language and Environment for Statistical Computing* (R Foundation for Statistical Computing, Vienna, 2014; www.R-project.org).
48. A. Zuur *et al.*, *Mixed Effects Models and Extensions in Ecology with R* (Springer, 2009).
49. J. A. Andrews, K. G. Harrison, R. Matamala, W. H. Schlesinger, Separation of root respiration from total soil respiration using carbon-13 labeling during free-air carbon dioxide enrichment (FACE). *Soil Sci. Soc. Am. J.* **63**, 1429 (1999). [doi:10.2136/sssaj1999.6351429x](https://doi.org/10.2136/sssaj1999.6351429x)
50. Q. Hua, M. Barbetti, A. Z. Rakowski, Atmospheric radiocarbon for the period 1950–2010. *Radiocarbon* **55**, 2059–2072 (2013). [doi:10.2458/azu\\_js\\_rc.v55i2.16177](https://doi.org/10.2458/azu_js_rc.v55i2.16177)
51. S. R. Saleska, J. Harte, M. S. Torn, The effect of experimental ecosystem warming on CO<sub>2</sub> fluxes in a montane meadow. *Glob. Change Biol.* **5**, 125–141 (1999). [doi:10.1046/j.1365-2486.1999.00216.x](https://doi.org/10.1046/j.1365-2486.1999.00216.x)
52. J. Harte, M. S. Torn, F.-R. Chang, B. Feifarek, A. P. Kinzig, R. Shaw, K. Shen, Global warming and soil microclimate: Results from a meadow-warming experiment. *Ecol. Appl.* **5**, 132–150 (1995). [doi:10.2307/1942058](https://doi.org/10.2307/1942058)
53. X. Lin, Z. Zhang, S. Wang, Y. Hu, G. Xu, C. Luo, X. Chang, J. Duan, Q. Lin, B. Xu, Y. Wang, X. Zhao, Z. Xie, Response of ecosystem respiration to warming and grazing during the growing seasons in the alpine meadow on the Tibetan plateau. *Agric. For. Meteorol.* **151**, 792–802 (2011). [doi:10.1016/j.agrformet.2011.01.009](https://doi.org/10.1016/j.agrformet.2011.01.009)

54. C. Luo, G. Xu, Z. Chao, S. Wang, X. Lin, Y. Hu, Z. Zhang, J. Duan, X. Chang, A. Su, Y. Li, X. Zhao, M. Du, Y. Tang, B. Kimball, Effect of warming and grazing on litter mass loss and temperature sensitivity of litter and dung mass loss on the Tibetan plateau. *Glob. Change Biol.* **16**, 1606–1617 (2010). [doi:10.1111/j.1365-2486.2009.02026.x](https://doi.org/10.1111/j.1365-2486.2009.02026.x)
55. Y. Luo, S. Wan, D. Hui, L. L. Wallace, Acclimatization of soil respiration to warming in a tall grass prairie. *Nature* **413**, 622–625 (2001). [doi:10.1038/35098065](https://doi.org/10.1038/35098065) Medline
56. X. Zhou, S. Wan, Y. Luo, Source components and interannual variability of soil CO<sub>2</sub> efflux under experimental warming and clipping in a grassland ecosystem. *Glob. Change Biol.* **13**, 661–775 (2007).
57. Y. Luo, R. Sherry, X. Zhou, S. Wan, Terrestrial carbon-cycle feedback to climate warming: Experimental evidence on plant regulation and impacts of biofuel feedstock harvest. *Glob. Change Biol. Bioenergy* **1**, 62–74 (2009). [doi:10.1111/j.1757-1707.2008.01005.x](https://doi.org/10.1111/j.1757-1707.2008.01005.x)
58. J. Zhou, K. Xue, J. Xie, Y. Deng, L. Wu, X. Cheng, S. Fei, S. Deng, Z. He, J. D. Van Nostrand, Y. Luo, Microbial mediation of carbon-cycle feedbacks to climate warming. *Nat. Clim. Chang.* **2**, 106–110 (2012). [doi:10.1038/nclimate1331](https://doi.org/10.1038/nclimate1331)
59. V. Suseela, R. T. Conant, M. D. Wallenstein, J. S. Dukes, Effects of soil moisture on the temperature sensitivity of heterotrophic respiration vary seasonally in an old-field climate change experiment. *Glob. Change Biol.* **18**, 336–348 (2012). [doi:10.1111/j.1365-2486.2011.02516.x](https://doi.org/10.1111/j.1365-2486.2011.02516.x)
60. W. Liu, Z. Zhang, S. Wan, Predominant role of water in regulating soil and microbial respiration and their responses to climate change in a semiarid grassland. *Glob. Change Biol.* **15**, 184–195 (2009). [doi:10.1111/j.1365-2486.2008.01728.x](https://doi.org/10.1111/j.1365-2486.2008.01728.x)
61. S. D. Allison, K. K. Treseder, Warming and drying suppress microbial activity and carbon cycling in boreal forest soils. *Glob. Change Biol.* **14**, 2898–2909 (2008). [doi:10.1111/j.1365-2486.2008.01716.x](https://doi.org/10.1111/j.1365-2486.2008.01716.x)
62. S. M. Niinistö, J. Silvola, S. Kellomäki, Soil CO<sub>2</sub> efflux in a boreal pine forest under atmospheric CO<sub>2</sub> enrichment and air warming. *Glob. Change Biol.* **10**, 1363–1376 (2004). [doi:10.1111/j.1365-2486.2004.00799.x](https://doi.org/10.1111/j.1365-2486.2004.00799.x)
63. D. Comstedt, B. Boström, J. D. Marshall, A. Holm, M. Slaney, S. Linder, A. Ekblad, Effects of elevated atmospheric carbon dioxide and temperature on soil respiration in a boreal forest using δ<sup>13</sup>C as a labeling tool. *Ecosystems* **9**, 1266–1277 (2006). [doi:10.1007/s10021-006-0110-5](https://doi.org/10.1007/s10021-006-0110-5)
64. S. Wan, R. J. Norby, J. Ledford, J. F. Weltzin, Responses of soil respiration to elevated CO<sub>2</sub>, air warming, and changing soil water availability in a model old-field grassland. *Glob. Change Biol.* **13**, 2411–2424 (2007). [doi:10.1111/j.1365-2486.2007.01433.x](https://doi.org/10.1111/j.1365-2486.2007.01433.x)

65. C. T. Garten Jr., A. T. Classen, R. J. Norby, Soil moisture surpasses elevated CO<sub>2</sub> and temperature as a control on soil carbon dynamics in a multi-factor climate change experiment. *Plant Soil* **319**, 85–94 (2009). [doi:10.1007/s11104-008-9851-6](https://doi.org/10.1007/s11104-008-9851-6)
66. E. Lellei-Kovács, E. Kovács-Láng, T. Kalapos, Z. Botta-Dukát, S. Barabás, C. Beier, Experimental warming does not enhance soil respiration in a semiarid temperate forest-steppe ecosystem. *Community Ecol.* **9**, 29–37 (2008). [doi:10.1556/ComEc.9.2008.1.4](https://doi.org/10.1556/ComEc.9.2008.1.4)
67. B. A. Emmett, C. Beier, M. Estiarte, A. Tietema, H. L. Kristensen, D. Williams, J. Peñuelas, I. Schmidt, A. Sowerby, The response of soil processes to climate change: Results from manipulation studies of shrublands across an environmental gradient. *Ecosystems* **7**, 625–637 (2004). [doi:10.1007/s10021-004-0220-x](https://doi.org/10.1007/s10021-004-0220-x)
68. C. Beier, B. Emmett, P. Gundersen, A. Tietema, J. Peñuelas, M. Estiarte, C. Gordon, A. Gorissen, L. Llorens, F. Roda, D. Williams, Novel approaches to study climate change effects on terrestrial ecosystems in the field: Drought and passive nighttime warming. *Ecosystems* **7**, 583–597 (2004). [doi:10.1007/s10021-004-0178-8](https://doi.org/10.1007/s10021-004-0178-8)
69. A. Schindlbacher, S. Zechmeister-Boltenstern, R. Jandl, Carbon losses due to soil warming: Do autotrophic and heterotrophic soil respiration respond equally? *Glob. Change Biol.* **15**, 901–913 (2009). [doi:10.1111/j.1365-2486.2008.01757.x](https://doi.org/10.1111/j.1365-2486.2008.01757.x)
70. L. E. Rustad, I. J. Fernandez, Experimental soil warming effects on CO<sub>2</sub> and CH<sub>4</sub> flux from a low elevation spruce-fir forest soil in Maine, USA. *Glob. Change Biol.* **4**, 597–605 (1998). [doi:10.1046/j.1365-2486.1998.00169.x](https://doi.org/10.1046/j.1365-2486.1998.00169.x)
71. D. R. Bronson, S. T. Gower, M. Tanner, S. Linder, I. Van Herk, Response of soil surface CO<sub>2</sub> flux in a boreal forest to ecosystem warming. *Glob. Change Biol.* **14**, 856–867 (2007). [doi:10.1111/j.1365-2486.2007.01508.x](https://doi.org/10.1111/j.1365-2486.2007.01508.x)
72. P. J. McHale, M. J. Mitchell, F. P. Bowles, Soil warming in a northern hardwood forest: Trace gas fluxes and leaf litter decomposition. *Can. J. For. Res.* **28**, 1365–1372 (1998). [doi:10.1139/x98-118](https://doi.org/10.1139/x98-118)
73. A. R. Contosta, S. D. Frey, A. B. Cooper, Seasonal dynamics of soil respiration and N mineralization in chronically warmed and fertilized soils. *Ecosphere* **2**, art36 (2011). [doi:10.1890/ES10-00133.1](https://doi.org/10.1890/ES10-00133.1)
74. W. T. Peterjohn, J. M. Melillo, P. A. Steudler, K. M. Newkirk, F. P. Bowles, J. D. Aber, Responses of trace gas fluxes and N availability to experimentally elevated soil temperatures. *Ecol. Appl.* **4**, 617–625 (1994). [doi:10.2307/1941962](https://doi.org/10.2307/1941962)
75. J. M. Melillo, S. Butler, J. Johnson, J. Mohan, P. Steudler, H. Lux, E. Burrows, F. Bowles, R. Smith, L. Scott, C. Vario, T. Hill, A. Burton, Y.-M. Zhou, J. Tang, Soil warming, carbon-nitrogen interactions, and forest carbon budgets. *Proc. Natl. Acad. Sci. U.S.A.* **108**, 9508–9512 (2011). [doi:10.1073/pnas.1018189108](https://doi.org/10.1073/pnas.1018189108) [Medline](#)

76. W. T. Peterjohn, J. M. Melillo, F. P. Bowles, P. A. Steudler, Soil warming and trace gas fluxes: Experimental design and preliminary flux results. *Oecologia* **93**, 18–24 (1993). [doi:10.1007/BF00321185](https://doi.org/10.1007/BF00321185)
77. I. P. Hartley, A. Heinemeyer, P. Ineson, Effects of three years of soil warming and shading on the rate of soil respiration: Substrate availability and not thermal acclimation mediates observed response. *Glob. Change Biol.* **13**, 1761–1770 (2007). [doi:10.1111/j.1365-2486.2007.01373.x](https://doi.org/10.1111/j.1365-2486.2007.01373.x)
78. P. Ineson, D. G. Benham, J. Poskitt, A. F. Harrison, K. Taylor, C. Woods, Effects of climate change on nitrogen dynamics in upland soils. 2. A soil warming study. *Glob. Change Biol.* **4**, 153–161 (1998). [doi:10.1046/j.1365-2486.1998.00119.x](https://doi.org/10.1046/j.1365-2486.1998.00119.x)